AIP | Applied Physics Letters

Effects of nanofluids containing graphene/graphene-oxide nanosheets on critical heat flux

Sung Dae Park, Seung Won Lee, Sarah Kang, In Cheol Bang, Ji Hyun Kim et al.

Citation: Appl. Phys. Lett. **97**, 023103 (2010); doi: 10.1063/1.3459971
View online: http://dx.doi.org/10.1063/1.3459971
View Table of Contents: http://apl.aip.org/resource/1/APPLAB/v97/i2
Published by the AIP Publishing LLC.

Effects of nanofluids containing graphene/graphene-oxide nanosheets on critical heat flux

Sung Dae Park,[1] Seung Won Lee,[1] Sarah Kang,[1] In Cheol Bang,[1,a)] Ji Hyun Kim,[1] Hyeon Suk Shin,[1] Dong Wook Lee,[1] and Dong Won Lee[2]
[1]*Interdisciplinary School of Green Energy, Ulsan National Institute of Science and Technology (UNIST), 100 Banyeon-ri, Eonyang-eup, Ulju-gun, Ulsan 689-798, Republic of Korea*
[2]*Korea Atomic Energy Research Institute, 1045 Daedeokdaero, Yuseong, Daejeon 305-353, Republic of Korea*

(Received 24 May 2010; accepted 11 June 2010; published online 13 July 2010)

The superb thermal conduction property of graphene establishes graphene as an excellent material for thermal management. In this paper, we selected graphene/graphene oxide nanosheets as the additives in nanofluids. The authors interestingly found that the highly enhanced critical heat flux (CHF) in the nanofluids containing graphene/graphene-oxide nanosheets (GON) cannot be explained by both the improved surface wettability and the capillarity of the nanoparticles deposition layer. Here we highlights that the GON nanofluid can be exploited to maximize the CHF the most efficiently by building up a characteristically ordered porous surface structure due to its own self-assembly characteristic resulting in a geometrically changed critical instability wavelength. © *2010 American Institute of Physics*. [doi:10.1063/1.3459971]

Nanofluids are colloidal dispersions of nanoparticles in a base fluid.[1] One of the most interesting characteristics of nanofluids is their capability to enhance the critical heat flux (CHF) significantly.[2,4] Since CHF is the upper limit of phase-change nucleate boiling heat transfer (BHT) as the most efficient heat transfer mode, such enhancement provides the potential for major performance improvement in many practical applications such as electronic chips and nuclear plants with ever higher-power-density with concerns of thermal management. For that reason, so far, many kinds of nanoparticles such as Al_2O_3, TiO_2, ZnO, and Au as well as Ag have been investigated for BHT and CHF. There is a consensus that such enhancement is related to buildup of deposition layer of nanoparticles during boiling of nanofluids.[3–6] In order to prove it, some researchers indirectly showed that deposition layer of nanoparticles improved both surface wettability and capillarity.[7,8] A question is rising on that there are no consideration of morphology of buildup of deposition layer by choosing some optimal nanoparticles with, for example, higher thermal conductivity, or better nanoparticle shape to enhance the CHF. Furthermore, the deposition layers should depend on the self-assembly characteristics of the nanomaterials. Therefore, the starting idea for the current work is to maximize CHF by adopting a material with better thermal conductivity and self-assembly characteristics to form a more beneficial structure to CHF enhancement.

Recently, there are a lot of interests about graphene, a single atomic layer thick, plane of carbon atoms arranged in a honeycomb lattice. Graphene's near room temperature thermal conductivity is in the range from 3500–5300 W/mK.[9] Therefore, it appears that the superb thermal conduction property of graphene establishes graphene as an excellent material for thermal management.[9] For that reason, we selected graphene and graphene oxide nanosheets as the additives of nanofluids to realize our staring idea regarding an optimal buildup-layer.

Graphene and graphene oxide nanofluids are prepared from graphite (powder size <45 μm). Modified Hummers method is used in preparing the graphene and graphene oxide nanofluids. The concentration of both graphene and graphene oxide nanofluid is 0.001 vol % (see the Fig. 1). Alumina nanofluids is also prepared with same concentration to compare the enhancement mechanisms in terms of the build-up layer structure. The boiling CHF experiments were performed through Joule heating method with nickel-chrome (80/20) wires.

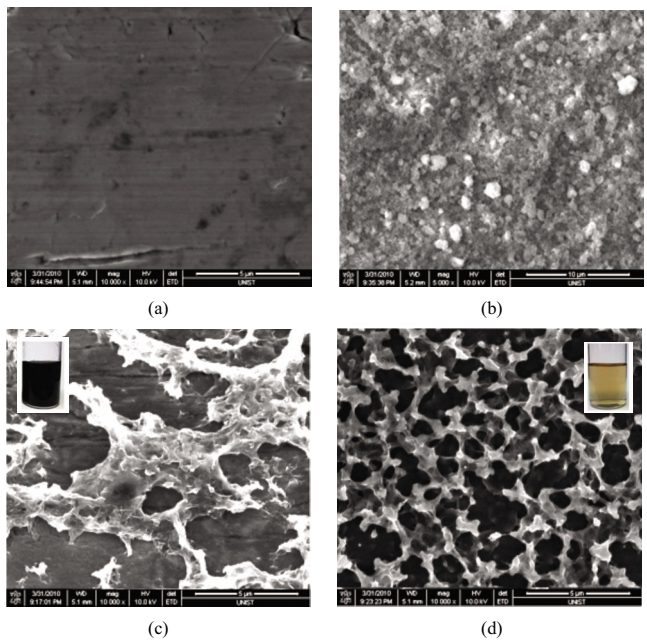

FIG. 1. (Color online) SEM image ($\times$10 000) of heater surface after pool boiling in (a) base-fluid water, (b) Al_2O_3 nanofluid, (c) graphene nanofluids, (d) graphene oxide nanofluid. (Insets in (c) and (d) are graphene and graphene oxide nanofluids, respectively).

a)Author to whom correspondence should be addressed. Electronic mail: icbang@unist.ac.kr. Tel.: +82-52-217-2915.

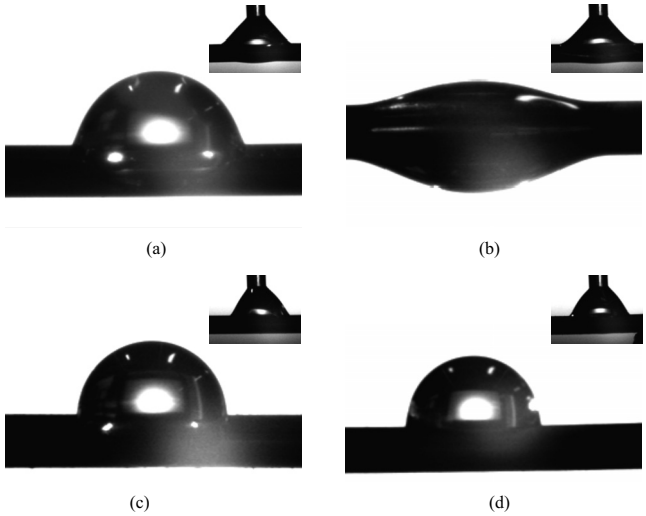

FIG. 2. Contact angle on tested wire surfaces with 1 μl water: (a) Bare wire (72°), (b) wire boiled in Al_2O_3 nanofluid (15°), (c) wire boiled in graphene nanofluid (82°), (d) wire boiled in graphene oxide nanofluid (85°); Insets show receding angle on tested wire surface with 1 μl water by contraction method (a) Bare wire (35°), (b) Al_2O_3 (22°), (c) graphene (50°), (d) graphene oxide (50°).

The graphene oxide nanofluid shows the largest CHF enhancement of 179%. The CHF of graphene nanofluid was 84% higher than CHF of pure water. Alumina nanofluid shows the 152% enhancement of CHF [see Fig. 4(a) for the CHF values of test fluids.]

After pool boiling experiments, build-up layers are observed on the heating surface. Figure 1 is the SEM images of heating wires which show the build-up layer structures. It is interesting that graphene-oxide nanofluid shows the build-up of a characteristically ordered porous structure compared to disordered deposition structure of alumina nanofluid and larger and less-ordered structure of graphene nanofluid. So far, CHF enhancement has been interpreted by change in the surface wettability and capillarity due to such deposition layers. Therefore, we investigated the surface wettability and capillarity of our surfaces to figure out the mechanisms of such enhancement, especially graphene oxide structure showing the highest CHF value. Initially, our expectation has been on the most improved surface wettability and capillarity. However, the result of observation of contact angle indicating the surface wettability was not on that. The contact angles of wires boiled in graphene oxide and graphene nanofluids are larger than one of bare wire boiled in pure water while the wire boiled in alumina nanofluid shows the well-known reduction in contact angle as shown in Fig. 2. In the following, the capillary wicking height ($L_c = 2\sigma \cos\theta/\rho g r$) was observed only for alumina nanofluid ($L_c = 1.21$ mm). Both graphene and graphene oxide nanofluids did not show any capillarity as shown in Fig. 3.

One of the well-known CHF prediction model considering a surface condition in terms of contact angle is Kandlikar's[10] CHF prediction model based on force balance on a bubble.

$$q''_{\mathrm{CHF}} = h_{fg}\rho_g^{1/2}\left(\frac{1+\cos\theta}{16}\right)\left[\frac{2}{\pi}+\frac{\pi}{4}(1+\cos\theta)\cos\varphi\right]^{1/2}[\sigma g(\rho_f-\rho_g)]^{1/4}, \quad (1)$$

where q''_{CHF} is the CHF, ρ_g is the gas density, ρ_f is the liquid density, h_{fg} is the latent heat from liquid state to gas state, σ is the surface tension, and θ, φ, and σ are receding contact angle, heater surface angle, and surface tension, respectively.

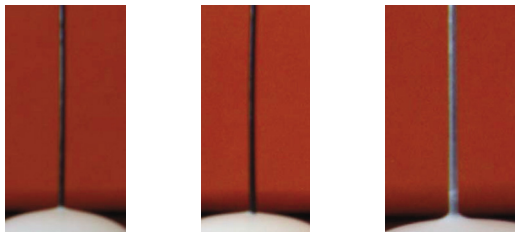

FIG. 3. (Color online) Capillary wicking height on tested wire surfaces with dye water (a) graphene oxide (No wicking: 0 mm), (b) graphene (No Wicking: 0 mm), (c) Al_2O_3 (1.21 mm). [One of the approaches to explain the CHF value enhancement is capillary wicking effect. Wicking structures which is causing the capillary phenomenon on heating surface promote to supply the water for delaying the dry out and cooling the dry spot (see Ref. 8). Figure 3 shows the result of capillary wicking effect on coated wires. In order to clearly display the boundary of liquid on wire, the white paint was used. Liquid rise was observed in only Al_2O_3 coated wire.]

When we checked the prediction model, the wettability or contact angle effect to CHF is basically based not on the advancing contact angle but on the receding contact angle (θ) because the growing bubble due to heat transfer from the surface physically causes the receding state of liquid on the surface. So, lastly we checked the receding angle for the surfaces as shown in Fig. 2.

While the effect of Al_2O_3 nanofluid could be explained by the improved surface wettability even with receding contact angle, however, interestingly, the enhancement of CHF for graphene/graphene oxide nanofluids could not be explained directly by the receding angle which has not been decreased but rather increased. Just in case, if the receding angle of 50° may be considered as hydrophilic angle (even though capillarity did not show reflection of such angle or no wicking height) and if we consider the complete wetting situation of Wendzel[11] on the porous structure with such hydrophilic case, we can add the effect of increase in effective liquid layer thickness to the Sadsivian's[12] macrolayer model (50° receding angle). It is the additional porous layer thickness considering the liquid-filled porous layer (porous layer volume:$\varepsilon 4 r_b^2 \delta_{\mathrm{porous}}$ where ε, r_b, and δ are porosity, bubble radius, and thickness, respectively).

$$\delta_{\mathrm{total}} = r_b\left[\cos\theta - \frac{\pi}{12}(3\cos\theta - \cos^3\theta)\right] + \varepsilon\delta_{\mathrm{porous}}, \quad (2)$$

$$q''_{\mathrm{CHF}} = \frac{\delta_{\mathrm{total}}\rho_f h_{fg}}{\tau_d}, \quad (3)$$

where q'', ρ_f, h_{fg}, and τ_d, are the heat flux, liquid density, evaporation heat, and time to dry out the macrolayer liquid film, respectively.

However, even in this case, the increase in the receding angle gives 150% decrease in CHF. Therefore, the CHF enhancement substantially should depend on the porous layer thickness.

We confirmed that it is very difficult to interpret the enhanced CHF of nanofluids containing graphene and GON by using the surface wettability and capillarity which have been responsible for CHF enhancement of the conventional nanofluids.

What is the reason why graphene/graphene oxide nanofluids show the CHF enhancement without such improved surface wettability and capillarity? We give an attention to the superb thermal conductivity of graphene or graphene oxide. Graphene oxide layer with higher thermal conductivity may assist in dissipating the hot spot by enhancing radial conduction on the surface. The effect of conduction in the heater[13] is typically described by the so-called "thermal activity," S as follows:

$$S = \delta\sqrt{\rho_h c_h k_h}, \tag{4}$$

which is the product of the heater characteristic dimension (δ) and the heater material effusivity ($\sqrt{\rho_h c_h k_h}$ where ρ_h, c_h, and k_h are density, specific heat, and thermal conductivity for heater material, respectively). The higher the thermal activity, the more effectively conduction can dissipate the hot/dry spot. The high-effusivity layer on the surface of the wire increases the heater thermal activity and thus can delay CHF.[14] The CHF enhancement for graphene and graphene oxide nanofluids may be interpreted as thermal dissipation improvement due to its higher effusivity. ($S_{\text{nichrome}} \sim 6,535, S_{\text{alumina}} \sim 11\ 100, S_{\text{graphene}} \sim 88\ 974$)

Next, we pay our attention to hydrodynamic instability theory or hydrodynamic liquid-choking limit again because there is an intriguing report to link the change in hydrodynamic instability wavelength into the CHF enhancement of a porous coating layer.[15]

The basic idea is that the hydrodynamic limit model based on Rayleigh–Taylor instability wavelength ($\lambda_{\text{RT,c}}$) on the plain surface originally proposed by Zuber[16] can be extended to a surface with microstructure coating and the capillary limit. The onset of CHF based on the hydrodynamic limit is due to the instability of vapor columns. The porous layer could change the critical distance between vapor columns on the heater and thus modify the critical instability wavelength. Liter and Kaviany[15] explained the effect of such modulation wavelength λ_m on CHF of a porous coating layer with the following equation:

$$q''_{\text{porous}} = \frac{\pi}{8} h_{fg} \left(\frac{\sigma \rho_g}{\lambda_m} \right)^{1/2}. \tag{5}$$

We checked the change in the wavelength by a simple experiment as shown in Fig. 4 (insets of photographs). Surprisingly the wavelength change corresponds to the CHF enhancement tendency for all tested nanofluids (alumina and graphene/graphene oxide) as shown in Fig. 4(b) compared to the effect of contact angle of Fig. 4(a).

The wavelength can be a geometrically determined factor according to the surface condition.[15] As the result, the change in wavelength prolongs the wetting of the surface by allowing the liquid to break through which means the enhancement of CHF. Recognizing that the CHF enhancement and wavelengths reported in the literature are not exactly matched with the prediction of Eq. (5), we can, however, conclude that the modulation of wavelength can sufficiently support the CHF enhancement of graphene/graphene oxide nanofluids compared to surface wettability and capillarity.

This work was supported by the Nuclear Research and Development Program through the National Research Foundation of Korea and the ITER development project funded by the Ministry of Education, Science and Technology.

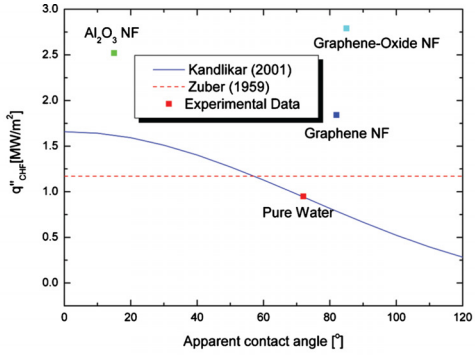

(a)

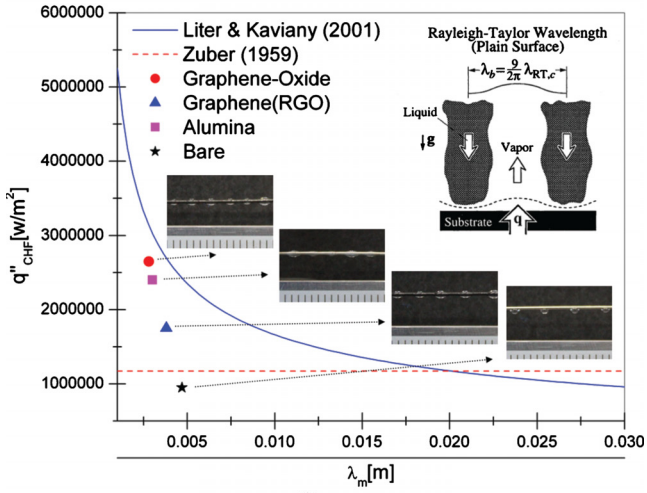

(b)

FIG. 4. (Color online) CHF phenomena and comparisons between models and experimental data. (a) Effects of a surface wettability (Kandlikar's model with contact angle), (b) Effects of a geometrically determined critical instability wavelength (Liter and Kaviany's model with modulation wavelength); Inset (illustration) shows Critical wavelength concept (base length scale λ_b on plain surface changes into λ_m on a porous surface, see Ref. 15). Insets of photographs show change in Rayleigh–Taylor instability on tested wire surfaces (geometrically determined critical instability wavelength). Graphene oxide wire (DIW, $\lambda_m \sim 2.8$ mm); Al_2O_3 wire (DIW, $\lambda_m \sim 3.0$ mm); graphene wire (DIW, $\lambda_m \sim 3.8$ mm); pure wire (DIW, $\lambda_m \sim 4.7$ mm).

[1] J. A. Eastman, S. U. Choi, S. Li, W. Yu, and L. J. Thompson, Appl. Phys. Lett. **78**, 718 (2001).
[2] S. M. You, J. H. Kim, and K. H. Kim, Appl. Phys. Lett. **83**, 3374 (2003).
[3] S. Das, N. Putra, and W. Roetzel, Int. J. Heat Mass Transfer **46**, 851 (2003).
[4] P. Vassallo, R. Kumar, and S. D'Amico, Int. J. Heat Mass Transfer **47**, 407 (2004).
[5] I. C. Bang and S. H. Chang, Int. J. Heat Mass Transfer **48**, 2407 (2005).
[6] D. Milanova and R. Kumar, Appl. Phys. Lett. **87**, 233107 (2005).
[7] S. J. Kim, I. C. Bang, J. Buongiorno, and L. W. Hu, Appl. Phys. Lett. **89**, 153107 (2006).
[8] H. Kim and M. Kim, Appl. Phys. Lett. **91**, 014104 (2007).
[9] http://www.nanowerk.com/spotlight/spotid=4641.php (2008).
[10] S. G. Kandlikar, J. Heat Transfer **123**, 1071 (2001).
[11] R. N. Wenzel, J. Phys. Colloid Chem. **53**, 1466 (1949).
[12] P. Sadasivan, P. R. Chappidi, C. Unal, and R. A. Nelson, *Pool and External Flow Boiling* (ASME, New York, 1992), p. 135.
[13] M. Arik and A. Bar-Cohen, Int. J. Heat Mass Transfer **46**, 3755 (2003).
[14] I. C. Bang, J. Buongiorno, L. W. Hu, and H. Wang, Journal of Power & Energy Systems **2**, 340 (2008).
[15] S. G. Liter and M. Kaviany, Int. J. Heat Mass Transfer **44**, 4287 (2001).
[16] N. Zuber, AECU-4439, (1959).